Materials Transactions, Vol. 44, No. 4 (2003) pp. 657 to 660

Microstructures and Mechanical Properties of Porosity-Graded Pure Titanium Compacts*[1]

Ik-Hyun Oh*[2], Haruhiko Segawa*[2], Naoyuki Nomura and Shuji Hanada

Institute for Materials Research, Tohoku University, Sendai 980-8577, Japan

Microstructures and mechanical properties of porosity-graded Ti compacts were investigated in this study. To fabricate the porosity-graded compacts, Ti powders with three different particle sizes, 65, 189 and 374 μm were prepared by the plasma rotating electrode process (PREP) and the gas atomization process, and these powders were sintered with and without applied stress. Porosity and pore size of porosity-graded Ti compacts decrease significantly with decreasing initial powder size and by applying stress. The most porous layer (374 μm) is severely deformed in compression tests compared to other layers. The compressive strength of porosity graded-compacts is found to be in fairly good agreement with the strength of most porous layer. Bend strength of compact sintered at 1223 K and 1 MPa (223.3 MPa) shows a higher value than that of human bone (156.9 MPa).

(Received December 5, 2002; Accepted February 6, 2003)

Keywords: *porosity graded, titanium powder sintering, porosity, pore size, 0.2% proof strength, bend strength*

1. Introduction

Metals and alloys are probably the most common materials used as surgical implants for artificial hard-tissue replacement.[1,2] Steinemann concluded that V, Ni, and Co asre toxic elements, while Ti and its alloys, stainless steels and CoCrMoNi alloys, and Ta, Zr, Nb, and Pt are 'resistant metallic biomaterials' based on corrosion rates.[1,3,4] Among various metallic biomaterials, pure Ti is most widely used because of its excellent corrosion resistance and high strength-to-weight ratio.[2,5,6] Most metallic biomaterials possess a critical issue related to the mismatch of Young's modulus between implant (110 GPa for Ti) and human bone (10–30 GPa).[7,8] One way to alleviate the problem is to reduce Young's modulus of pure Ti by introducing pores, thereby minimizing damages to tissues adjacent to the implant.[8,9] Recently, Oh *et al.* have measured Young's modulus of porous Ti compacts which have various porosities, fabricated by several sintering conditions.[8] They reported that Young's modulus of porous Ti compacts with porosity of 32–35 vol% is similar to that of human bone.

Considering the application of porous Ti as bone, integration to the other kind of bone or joining to the other functional components such as arthro is inevitable. In this case, materials properties of porous Ti should be changed gradually toward the jointed part. We have tried to fabricate porosity-, strength- and modulus-graded porous Ti, as one of the newly designed functional materials for biomedical applications. Microstructures and mechanical properties of porosity-graded Ti compacts are mainly investigated in this study.

2. Experimental Procedure

Ti powders with three different particle sizes were prepared from the plasma rotating electrode process (PREP) and the gas atomization process in an Ar atmosphere. The PREP powders were atomized from pure Ti (grade 2). The parameters of PREP are described elsewhere.[8] The PREPed powders were sieved to use similar sizes of particles in the range of about 300–500 μm with a mean diameter 374 μm. The purity of Ti powders is 99.9 mass%. Commercially available gas atomized Ti powders with a high purity of 99.9% (Sumitomo Titanium Corp.) were also sieved in the range of about 150–250 μm (mean 189 μm) and 45–150 μm (mean 65 μm).

To fabricate porosity-graded compacts, Ti powders with three different particle sizes were carefully stacked in the order of the powders 65, 189 and 374 μm between two graphite punches in a graphite mold of 30 mm diameter. BN lubricant was sprayed on the graphite punches and inner wall of the mold to avoid the reaction between carbon and Ti during sintering. To attain uniform compaction of the powders, the stacked powders were pre-pressed at 70 MPa for 0.6 ks. After that, they were sintered in a vacuum of 1×10^{-3} Pa at two conditions; (1) 1573 K without pressure for 7.2 ks and (2) 1223 K with uniaxial pressure of 1 MPa for 7.2 ks.

Microstructures of porosity-graded compacts were observed with an optical microscope (OM) and a scanning electron microscope (SEM). Specimens for the observation were polished with SiC paper up to #3000, and then vibratorily polished in a Buehler Vibormet 2 with 0.3 μm Al_2O_3. To measure the porosity of each layer in the porosity-graded compacts, layers were cut using an electro discharge machine and polished carefully using a SiC paper. The divided layers are finally finished into rectangular shape. The porosity was evaluated from the weight and the apparent volume of the specimen. Pore size was calculated by the mean value of 50 individual pore length measurements on each layer in the graded compacts. Mechanical properties of the graded compacts were evaluated using compression test and three-point bending test at room temperature. The 0.2% proof strength ($\sigma_{0.2}$) was evaluated in the compression test using rectangular shaped sample with the size of $3.5 \times 3.5 \times 21\,mm^3$. The height of each layer was 7 mm.

*[1]This Paper was Presented at the Fall Meeting of the Japan Institute of Metals, held in Osaka, on November 2, 2002.
*[2]Graduate student, Tohoku University.

The compression test was stopped before the sample was buckled. The bend strength (σ_B) was evaluated at a peak stress in the load-displacement curve. σ_B was calculated using the following equation; $\sigma_B = 3PL/2wt^2$, where P is maximum load applied, L is span length, and w and t are width and thickness of specimen, respectively. Three-point bending test was carried out using a rectangular bar with the size of $6 \times 6 \times 27\,mm^3$ with length of 9 mm in each layer. Bending load was applied at the center of the bar, consisting of medium porosity layer, as supported by both the layers having maximum and minimum porosites. The span length was 24 mm.

3. Results and Discussion

3.1 Morphology of Ti powders

Figure 1 shows SEM micrographs of Ti powders produced by PREP (Fig. 1(a)) and gas atomization process (Figs. 1(b) and (c)), respectively. The PREPed powder is entirely spherical in shape and possesses a smooth surface, as shown in Fig. 1(a). On the other hand, the gas atomized powders have small adhering satellites (Figs. 1(b) and (c)). It is generally known that metal powder formation by gas atomization involves the break-up of liquid stream by the rapidly expanding gas. Because of a suction pressure in the gas expansion zone, the liquid stream first forms into a thin hollow sheet, and subsequently forms ligaments, ellipsoids, and sphere. Consequently, the solidified small particles are carried into the flight path of the molten large droplets, resulting in agglomeration and satellites.[10)]

3.2 Microstructure of porosity-graded Ti compacts

Table 1 summarizes the porosity and pore size of porosity-graded Ti compacts sintered at 1573 K and 1223 K with a pressure of 1 MPa (abbreviated hereafter as 1573 K and 1223 K/1 MPa). They are gradually decreased with decreasing initial powder size. Figure 2(a) shows OM micrograph of polished cross-section of porosity-graded Ti compact sintered at 1223 K with a pressure of 1 MPa (abbreviated hereafter as 1223 K/1 MPa). Porosity-graded compact is found to be successfully sintered, consisting of three layers of porous Ti. Powders (light contrast) and pore (dark contrast) are homogeneously distributed in each layer. Also, no detectable crack and defect at interface of compact can be seen in each layer. Interparticle boundaries were readily distinguished in 374 μm layer. According to our previous report, porous Ti compact containing the porosity of 26.3%, which was sintered using Ti powder with the same particle size (374 μm), has the open porosity of 95.3%.[8)] It is considered that most of pore in the 1223 K/1 MPa would be connected each other in the layer. On the other hand, shape of the pore was spherical and interparticle boundaries were not well discernible in 65 μm layer, as shown in Fig. 2(b). These results clearly show that porosity and pore size are controllable by changing the diameter of Ti powders. This porosity difference is attributed to the surface energy per unit volume, which depends on the inverse of the particle diameter. Thus, smaller particles with high specific surface area have more energy, so that they could be sintered faster.

The porosity and the pore size in each layer of compact at 1223 K/1 MPa show lower values, compared to those of compact at 1573 K. This would be due to the low strength of pure Ti above β phase transition temperature (1156 K). Stress concentration occurring at point contacts between powders could deform Ti powders at the contacts preferentially, thereby leading to the densification of Ti compacts. Therefore, it is considered that applying pressure of 1 MPa is more effective to fabricate dense Ti compacts than increasing the sintering temperature up to 1573 K.

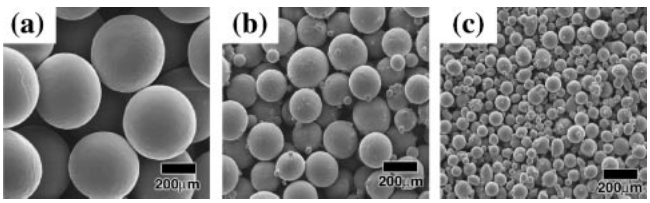

Fig. 1 SEM micrographs of starting Ti powders with different particle sizes in the range of (a) 300–500 μm (PREP), (b) 150–250 μm (gas atomization) and (c) 45–150 μm (gas atomization).

Table 1 Porosity and mean pore size of each layer for the porosity-graded Ti compacts sintered at 1573 K and 1223 K with the pressure of 1 MPa.

	1573 K		1223 K/1 MPa	
	Porosity (%)	Mean pore size, r/μm	Porosity (%)	Mean pore size, r/μm
65 μm layer	28.3	19.9	9.8	17.9
189 μm layer	33.1	73.1	19.8	58.4
374 μm layer	35.5	154.3	24.8	117.5

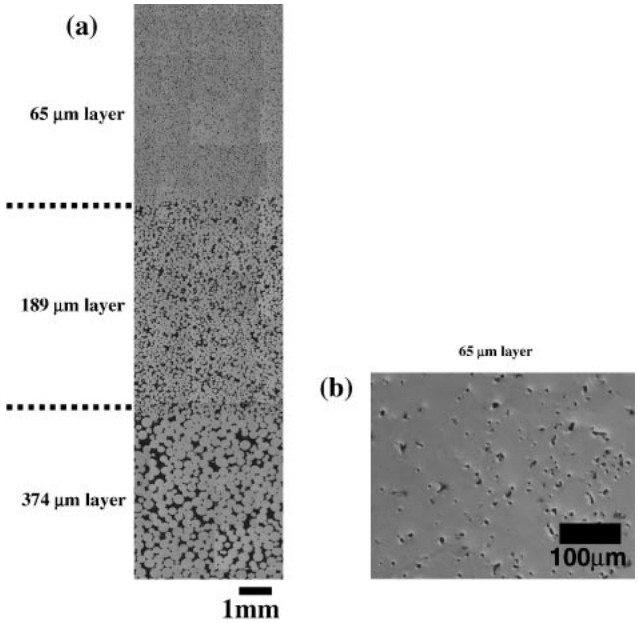

Fig. 2 OM micrograph of porosity-graded Ti compact with three layers sintered at 1223 K with the pressure of 1 MPa. (a) three layers (374 μm, 189 μm and 65 μm) compact and (b) high magnification view of 65 μm layer.

3.3 Mechanical properties

3.3.1 Compression test

0.2% proof strength ($\sigma_{0.2}$) of the porosity-graded compacts sintered at 1573 K and 1223 K/1 MPa is 22.3 and 106.8 MPa, respectively. It is obvious that more porous Ti compact (1573 K) shows lower strength than dense compact (1223 K/1 MPa). Figure 3 shows strain-stress curves obtained by compression test for the porosity-graded compacts which were sintered at 1573 K and 1223 K/1 MPa. Although these compacts were deformed to plastic strain of 3.5%, load drops and buckling were not observed.

Figure 4 shows deformation microstructure of compact at 1223 K/1 MPa in each layer after compression test at the plastic strain of 3.5%. The 374 µm particle layer (see Fig. 4(a)) is severely deformed compared to other layers (Figs. 4(b) and (c)). The deformation microstructure of compact at 1573 K showed the same tendency as the compact at 1223 K/1 MPa. The present authors have previously reported the porosity dependence of 0.2% proof strength of various porous Ti compacts, which were sintered using Ti powders of the average diameter of 374 µm.[8] The strength of porous Ti compacts ($\sigma_{0.2}$) can be estimated with liner fitting as follows;

$$\sigma_{0.2} = -9.41 \times V_p + 350 \quad (1)$$

Here, V_p is the porosity (%) of Ti compacts. Assuming $V_p = 0$, eq. (1) yields 350 MPa as the strength of porosity-free pure Ti (grade 2). This value is in reasonable agreement with the 0.2% proof strength of pure Ti (grade 2) defined by ASTM,[11] being in the range from 275 to 450 MPa. Using this equation, the strength of the most porous layer is calculated as 15.9 MPa ($V_p = 35.5$) and 116.6 MPa ($V_p = 24.8$). These values are consistent with the average 0.2% proof strength of porosity-graded compacts. Therefore, the compressive strength can be controlled by the strength of the most porous layer in the compact. In other words, deformation of the porosity-graded compacts could initiate at the 374 µm particle layer and proceed toward lower porosity layer.

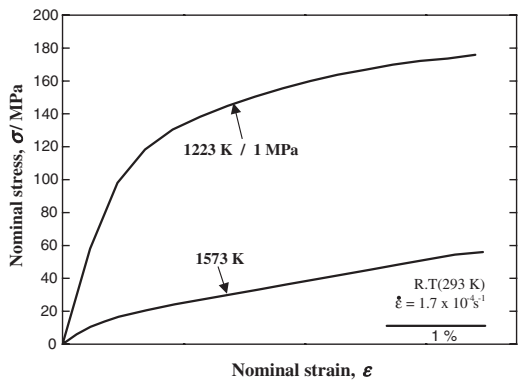

Fig. 3 Stress-strain curves after compressive test for the porosity-graded Ti compacts sintered at 1573 K and 1223 K with the pressure of 1 MPa.

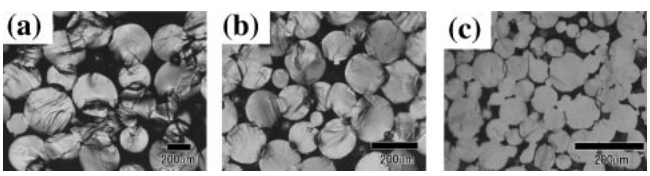

Fig. 4 OM micrographs of each layer after compression test for the porosity-graded Ti compact sintered at 1223 K with the pressure of 1 MPa. This specimen was deformed up to 3.5% at room temperature. (a) mean particle size 374 µm layer, (b) mean particle size 189 µm layer and (c) mean particle size 65 µm layer.

3.3.2 Three-point bending test

Figure 5 shows load-displacement curves obtained by three-point bending test for the porosity-graded compacts. Load drops were observed after showing linear elastic behavior followed by non-linear deformation up to a peak load. No catastrophic fracture was caused for both compacts. Therefore, plastic deformation of porosity-graded compacts would be achieved in neck regions. Bend strength of the porosity-graded compacts sintered at 1573 K and 1223 K/1 MPa is 40.9 and 223.3 MPa, respectively. Bend strength of compact at 1223 K/1 MPa is higher than that of human bone (156.9 MPa),[12] although the compact at 1573 K shows a considerably lower value. Figure 6 shows OM microstructures of the porosity-graded compacts after bend test. These were taken from the lateral and bottom surfaces of the bending specimens. Main crack initiation layer is noticeably different in both graded compacts. In the compact at 1223 K/1 MPa, a main crack initiates and propagates along the particle boundaries in the middle (189 µm) layer, where the pin for bending load is located, as shown in Figs. 6(a) and (b). On the other hand, a main crack in the compact at 1573 K ((Figs. 6(c) and (d)) is generated within the 374 µm layer having maximum porosity, although the pin is placed at a 189 µm layer. Maximum tensile stress for three-point bending test is usually generated on the back of the load point. It is likely that the middle layer (189 µm) can endure the maximum stress during bending, while the 374 µm layer cannot. It should be noted that fracture does not occur at the interface between 189 µm and 374 µm layers. This indicates that the interface strength could be higher than that of the monolithic 374 µm layer. When the porosity-graded Ti compact is fabricated by the powder stacking method using 189 µm and 374 µm powders, the contact number at interface between 189 µm and 374 µm particles is found to be more than that in 374 µm layer, in shown Fig. 6(d). In other words, the density of stacked powders with the different diameters of

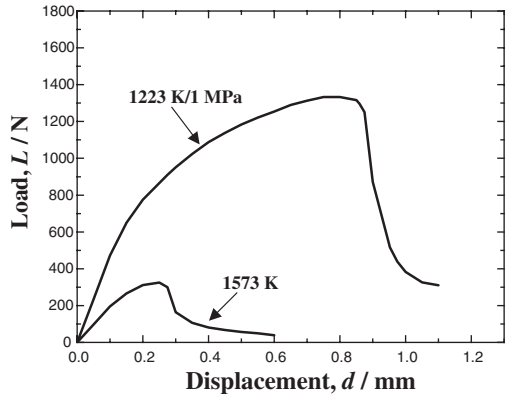

Fig. 5 Load-displacement curves after three-point bending test for the porosity-graded Ti compacts sintered at 1573 K and 1223 K with the pressure of 1 MPa.

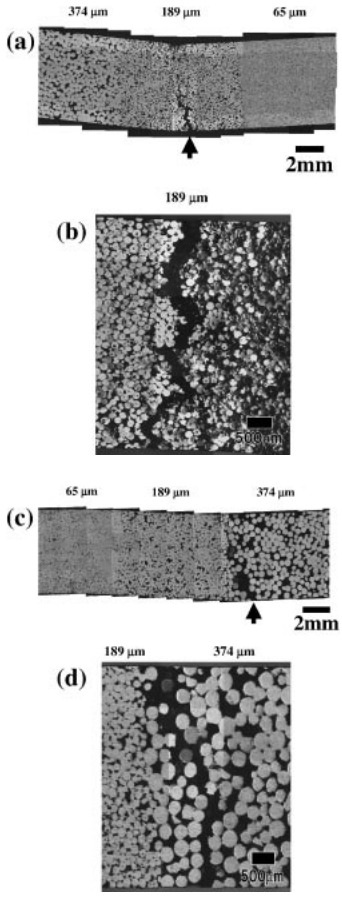

Fig. 6 OM micrographs of main crack generated layer after three-point bending test for porosity-graded Ti compacts. (a) lateral surface of compact sintered at 1223 K with the pressure of 1 MPa, (b) bottom surface of compact sintered at 1223 K with the pressure of 1 MPa, (c) lateral surface of compact sintered at 1573 K and (d) base surface of compact sintered at 1573 K.

189 and 374 μm is higher than that of stacked powder with only the diameter of 374 μm, because small particles can fill pores between large particles. Therefore, the interface strength of 189 μm and 374 μm layer is presumably higher than that of 374 μm layer. Further examination is needed to clarify the interfacial strength for the porosity-graded compacts. Also, stress analysis of porosity-graded layer would be needed to determine the layer thickness to avoid the fracture at lower strength in higher porosity layer using finite element analysis.

In summary, synthesis of porosity-graded Ti compact, which allows porous Ti to be applied to biomedical devices, is demonstrated in this study. Thus, porosity-graded Ti compacts will be applicable to biomaterials when its joining condition to other devices as well as the layer number and thickness is optimized for the practical implants.

4. Conclusions

Porosity-graded Ti compacts with three layers were successfully fabricated by sintering PREPed and gas atomized Ti powders in this study. The microstructures and mechanical properties were investigated. The results obtained are summarized as follows:

(1) Porosity and pore size of porosity-graded Ti compact decrease with decreasing the initial powder size and by applying the pressure.
(2) The most porous layer (374 μm) is severely deformed compared to other layers in compression tests.
(3) The compressive strength of porosity-graded compacts is found to be in fairly good agreement with the strength of most porous layer.
(4) Bend strength of compact at 1223 K/1 MPa (222.3 MPa) shows a higher value than that of human bone (156.9 MPa).
(5) Main crack is observed in the middle (189 μm) layer in the compact at 1223 K/1 MPa, while it is generated within the 374 μm layer having maximum porosity in the compact at 1573 K.

Acknowledgements

The authors are grateful to S. Watanabe and T. Abumiya for technical discussion. The present work was supported by a Grant-in Aid for Scientific Research on Priority Area (No. 11221202) from the Ministry of Education, Culture, Sports, Science and Technology, Japan.

REFERENCES

1) B. Y. Li, L. J. Rong, Y. Y. Li and V. E. Gjunter: Acta Mater. **48** (2000) 3895–3904.
2) D. Kuroda, M. Niinomi, M. Morinaga, Y. Kato and T. Yashiro: Mater. Sci. Eng. **A243** (1998) 244–249.
3) M. Long and H. J. Rack: Biomaterials **19** (1998) 1621–1639.
4) S. G. Steinemann: Titanium'84 Science and Technology **2** (1985) 1373–1379.
5) K. H. W. Seah, R. Thampuran and S. H. Teoh: Corros. Sci. **40** (1998) 547–556.
6) Y. Okazaki, E. Nishimura, H. Nakada and K. Kobayashi: Biomatreials **22** (2001) 599–607.
7) C. E. Wen, M. Mabuchi, Y. Yamada, K. Shimojima, Y. Chino and T. Asahina: Scr. Mater. **45** (2001) 1147–1153.
8) I. H. Oh, N. Nomura and S. Hanada: Mater. Trans. **43** (2002) 443–446.
9) D. J. Blackwood, A. W. C. Chua, K. H. W. Seah, R. Thampuran and S. H. Teoh: Corros. Sci. **42** (2000) 481–503.
10) R. M. German: *Powder metallurgy science*, (Metal powder industries federation, Prsnceton, New Jersey, 1994) pp. 84–125.
11) R. Boyer, G. Welsch and E. W. Collings: *Materials properties handbook: Titanium alloys*, (ASM International, Materials Park, OH, 1994) pp. 165.
12) H. Yamada: *Strength of Biological Materials*, (The Williams & Wilkins Company, Baltmore, Maryland, 1970) pp. 19–105.